

# Hot-electron noise suppression in n-Si via the Hall effect

**Francesco Ciccarello**

CNISM and Dipartimento di Fisica e Tecnologie Relative dell'Università degli Studi di Palermo, Viale delle Scienze, Edificio 18, I-90128 Palermo, Italy

E-mail: ciccarello@difter.unipa.it

**Salvatore Zammito**

CNISM and Dipartimento di Fisica e Tecnologie Relative dell'Università degli Studi di Palermo, Viale delle Scienze, Edificio 18, I-90128 Palermo, Italy

**Michelangelo Zarcone**

CNISM and Dipartimento di Fisica e Tecnologie Relative dell'Università degli Studi di Palermo, Viale delle Scienze, Edificio 18, I-90128 Palermo, Italy

**Abstract.** We investigate how hot-electron fluctuations in n-type Si are affected by the presence of an intense (static) magnetic field in a Hall geometry. By using the Monte Carlo method, we find that the known Hall-effect-induced redistribution of electrons among valleys can suppress electron fluctuations with a simultaneous enhancement of the drift velocity.

PACS numbers:

## 1. Introduction

The study of hot-electron transport properties of semiconductor materials has witnessed impressive progresses in the last decades. Clearly, these have been motivated by the well-known technologic relevance of semiconductors, together with the unceasing miniaturization process of electronic devices. In semiconductor micro-devices electrons may be accelerated by electric fields of the order of even several kV/cm, so the transport is in general highly non-ohmic and deviations from thermal equilibrium are significant. Mainly due to the formidable mathematical difficulties in solving the Boltzmann equation in such cases, the Monte Carlo (MC) method for the direct simulation of charge carriers' motion became what is probably the most popular numerical tool for approaching problems of this sort [1]. While most of the studies in this area focused on transport in the presence of electric fields, some MC investigations addressed the case where both an electric and a magnetic field are present in compounds such as GaAs

[2, 3, 4], InSb [5, 6, 7, 8], Si [10] and GaN [9]. In particular, two of us have recently investigated hot-electron noise in n-GaAs in the Hall geometry for electric fields of the order of some kV/cm and magnetic-field strengths up to 2 T [4]. The presence of the magnetic field was shown to affect the electron-velocity autocorrelation function and the noise spectrum of velocity fluctuations in a non-trivial way. In particular, the magnetic field was shown to give rise to an attenuation of electron fluctuations around the drift velocity for electric-field strengths intense enough to yield a significant population of  $L$ -valleys [4].

In a multivalley semiconductor, a significant contribution to nonlinearity comes from the carriers' distribution among valleys with different effective masses. This is also true when all the valleys are energetically equivalent but, due to conduction-band anisotropy such as in Si, they have different mass tensor. The electron heating by the applied electric field is higher in valleys with lower mass along the field direction and thus such hot valleys are less populated. However, if a magnetic field is added to the applied electric field according to a Hall geometry, the above behaviour can be reversed: the hot (cold) valleys in the zero-magnetic-field case now become the cold (hot) ones. Such effect was demonstrated long ago in n-Si at  $T=77$  K, both experimentally and theoretically, and shown to be able to enhance conductivity [12]. To the best of our knowledge, however, no analysis of how electron velocity fluctuations are affected was carried out so far. Regardless, the problem is physically intriguing. Indeed, it is well-known that the application of a static electric field along crystallographic directions such as  $\langle 100 \rangle$  (or equivalent ones) in n-Si give rise to the so called *partition noise*: Electrons in valleys with different effective masses along the field direction have also different average velocities. As the drift velocity has of course an intermediate value, this implies an extra amount of velocity fluctuations. The typical signature of such phenomenon is the presence of a long-time tail in the longitudinal autocorrelation function of velocity fluctuations (whose length is dictated by the  $f$ -type intervalley scattering rate) [13, 14, 15]. The main motivation behind this work is to establish whether in a Hall geometry the aforementioned Hall-effect-induced redistribution of electrons among different valleys is able to attenuate partition noise.

When, in addition to the electric field, a perpendicular magnetic field is also applied, two main effects occur. First, the free-flight electron motion in the momentum space now takes place along closed orbits and thus the amount of gainable energy in a given free-flight is upper-bounded [2, 4]. Second, the Hall field adds to the applied electric field and at strong enough magnetic fields the former may even exceeds the latter. In a multivalley semiconductor, both the magnetic and the Hall fields can in general be sensed differently by electrons moving in different valleys and thus the conduction properties in the hot-electron regime may be significantly affected [12]. Here, we shall show that the drift-velocity enhancement shown in Ref. [12] may occur with a simultaneous decrease of velocity fluctuations and partition noise.

This paper is organized as follows. In Sec. 2, we describe the model and parameters used for the conduction band of n-Si and the various scattering processes as well as the

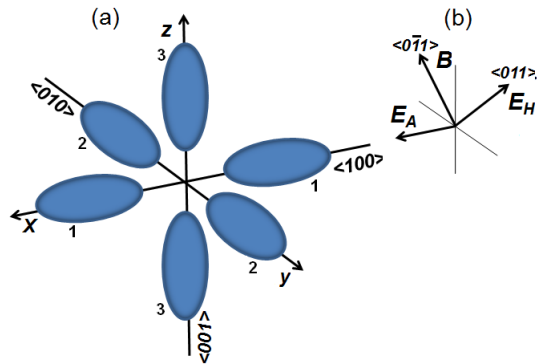


**Figure 1.** (a) Sketch of the valleys 1, 2 and 3 along the crystallographic directions  $\langle 100 \rangle$ ,  $\langle 010 \rangle$  and  $\langle 001 \rangle$ , respectively. (b) Hall geometry with  $\mathbf{E}_A$ ,  $\mathbf{E}_H$  and  $\mathbf{B}$  along the crystallographic directions  $\langle 100 \rangle$ ,  $\langle 011 \rangle$  and  $\langle 0\bar{1}1 \rangle$ , respectively.

approach we followed to tackle the problem. Sec. 3 is devoted to the central result of this work, i.e. the reduction of partition noise and of the relative importance of velocity fluctuations compared to the drift velocity. Additional plots illustrating the mechanism behind are presented and discussed. Finally, in Sec. 4 we draw our conclusions and outline the open problems.

## 2. Model and approach

We have modeled the conduction band of Si as three pairs of nonparabolic ellipsoidal valleys along the  $\langle 100 \rangle$ ,  $\langle 010 \rangle$  and  $\langle 001 \rangle$  directions, to be referred to as valleys 1, 2 and 3, respectively [see Fig. 1(a)]. The  $\langle 100 \rangle$ ,  $\langle 010 \rangle$  and  $\langle 001 \rangle$  directions are taken as the  $x$ ,  $y$  and  $z$ -axis, respectively, of the reference frame here adopted [see Fig. 1(a)]. For each valley, we take as longitudinal and transverse effective masses  $m_l = 0.916 m_0$  and  $m_t = 0.19 m_0$ , respectively, and nonparabolicity factor  $\alpha = 0.5 \text{ eV}^{-1}$ . We have included six intervalley-phonon scattering processes, three of  $f$ -type and three of  $g$ -type, as well as acoustic intravalley scattering [11] with the associated phonon equivalent temperatures and potentials used in Ref. [14]. Assuming a pure enough sample, no impurity scattering has been included [14].

The MC procedure for tackling hot-electron transport in crossed electric and magnetic fields in a semiconductor bulk was first suggested by Boardman *et al.* [2] and used in Ref. [4] for the case of GaAs. The basic idea is to derive the Newtonian time-evolution of the electron wave vector  $\mathbf{k}(t)$  during free flights in the presence of the static magnetic field  $\mathbf{B}$  and the *total* electric field  $\mathbf{E}$ . Unlike in the absence of magnetic field, the latter is the superposition of the applied electric field and the Hall field according to  $\mathbf{E} = \mathbf{E}_A + \mathbf{E}_H$ . To overcome the difficulty that for set values of  $\mathbf{E}_A$  and  $\mathbf{B}$  the Hall field  $\mathbf{E}_H$  is initially unknown, the total electric field  $\mathbf{E}$  is used as an independent parameter, together with  $\mathbf{B}$ , and the simulation is run in order to compute the drift velocity  $\mathbf{v}_d$ . The component of the total electric field  $\mathbf{E}$  along (orthogonal to) the direction of  $\mathbf{v}_d$  yields

$\mathbf{E}_A$  ( $\mathbf{E}_H$ ) [2]. This simple approach is fruitful in the case of isotropic materials (such as GaAs), when the transport properties depend solely on the magnitude of  $\mathbf{E}$ . However, due to electron-mass anisotropy, the procedure cannot be adopted in materials such as Si where  $\mathbf{v}_d$  depends on the direction of the electric field as well [10]. In our analysis we thus treated both  $E_A$  and  $E_H$ , i.e. the two components of  $\mathbf{E}$  in the plane orthogonal to  $\mathbf{B}$ , as independent parameters of the MC simulation. For given  $E_A$  and  $B$ , different simulations were run, each with a different value of  $E_H$ . The correct Hall field is the one yielding  $\mathbf{v}_d$  along  $\mathbf{E}_A$  [10]. Regarding the Hall geometry, in this work we address the case where  $\mathbf{E}_A$ ,  $\mathbf{E}_H$  and  $\mathbf{B}$  lie along the crystallographic directions  $\langle 100 \rangle$ ,  $\langle 011 \rangle$  and  $\langle 0\bar{1}1 \rangle$ , respectively [see Fig. 1(b)]. Such geometry has the advantage that the fields are symmetric with respect to valleys 2 and 3 and thus such groups of valleys necessarily exhibit the same behaviour. This will simplify our discussion.

The time-evolution of the electron wave vector in a given valley during a free flight is governed by the Newton's law

$$\hbar \dot{\mathbf{k}} = e [\mathbf{E} + \mathbf{v}(\mathbf{k}) \times \mathbf{B}], \quad (1)$$

where  $\mathbf{v}(\mathbf{k}) = \frac{1}{\hbar} \nabla_{\mathbf{k}} \varepsilon(\mathbf{k})$  is the electron group velocity and the energy-wave vector relationship that accounts for nonparabolicity effects is [16]  $\varepsilon(1 + \alpha\varepsilon) = \hbar^2/2 (k_l^2/m_l + k_t^2/m_t)$  [ $k_l$  ( $k_t$ ) are the longitudinal (transverse) components of the wave vector]. In order to fully account for the nonparabolicity effects which are rather important in Si [11], Eq. (1) has been solved numerically at each free flight. Despite Eq. (1) has no trivial analytic solution, some qualitative predictions can be established. Indeed, it is clear that, similarly to the isotropic case [2], the free-flight electron motion in the momentum space takes place along closed orbits around a displaced center. In the isotropic case the period of motion is dictated by the cyclotron frequency  $\omega_c = eB/m^*$  [2, 4]. Here, due to band anisotropy which implies the presence of the two effective masses  $m_l$  and  $m_t$ , two cyclotron frequencies are exhibited. In addition, unlike the circular nature of motion in the isotropic case, in the present case the orbits are in general elliptical.

As the fields are static and we are concerned with steady-state transport in bulk *n*-Si, the results presented in this work were obtained by simulating single-particle time-histories for times up to  $\mu\text{s}$ . The treatment of the scattering processes was performed in the usual way [1]. In this paper, we consider electric fields of the order of some kV/cm and magnetic-field strengths of the order of some T. We have checked that the product between the cyclotron frequencies and the typical electron relaxation time exhibits moderate values, which justifies that the magnetic-field strengths here considered do not give rise to quantum effects as we have assumed.

Finally, both the drift velocity  $v_d$  and the variance of velocity fluctuations  $\langle \delta v^2 \rangle$  were computed from a sampling of the electron velocity along the applied-electric-field direction. The results presented in this paper were obtained by setting the temperature to 77 K.

### 3. Noise suppression

In Fig. 2 we plot the drift velocity  $v_d$  (a), the variance  $\langle \delta v^2 \rangle$  (b) and the relative standard deviation  $\sqrt{\langle \delta v^2 \rangle}/v_d$  (c), respectively, against the magnetic field strength for  $E_A=6, 10$  kV/cm. Notice that, for a given applied electric field, the drift velocity  $v_d$  grows

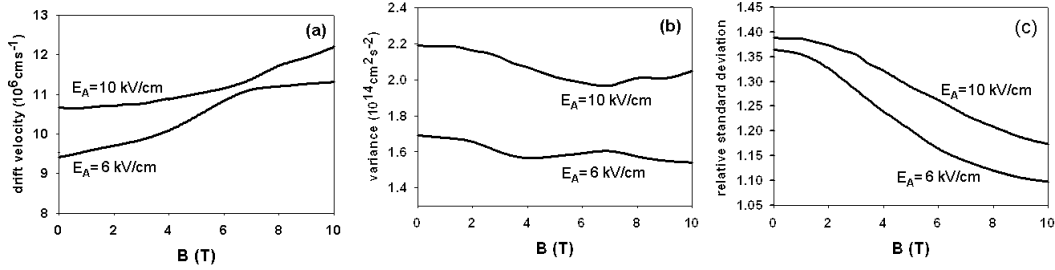


**Figure 2.** (a) Drift velocity  $v_d$  ( $10^6$  cm/s) vs. magnetic field  $B$ . (b) Velocity variance  $\langle \delta v^2 \rangle$  ( $10^{14}$  cm<sup>2</sup>/s<sup>2</sup>) vs.  $B$ . (c) Relative standard deviation  $\sqrt{\langle \delta v^2 \rangle}/v_d$  vs.  $B$ . The set values of the applied electric field are  $E_A=6, 10$  kV/cm.

with  $B$ , which confirms the magnetic-field-induced increase of conductivity predicted in Refs. [12]. Such interpretation is strengthened by the behaviour of the populations and mean energies of the three group of valleys for increasing values of  $B$  plotted in Figs. 3 (a) and (b), respectively, in the case  $E_A=6$  kV/cm. At low magnetic fields,

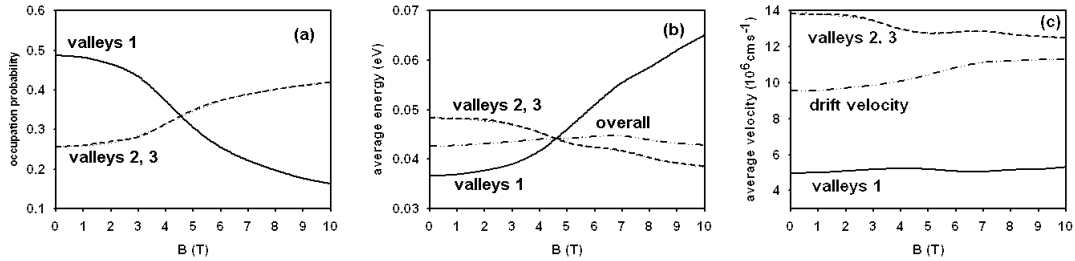


**Figure 3.** (a) Valley occupation probabilities vs. magnetic field  $B$ . (b) Valley average energy and overall average energy vs.  $B$ . (c) Valley average velocities along the applied electric field and drift velocity vs.  $B$ . We have set the applied-electric-field strength to  $E_A=6$  kV/cm.

when the dominating effect is that due to the electric field, valleys 1 are the coldest, and thus the most populated, given that they have the largest effective mass along the applied electric field  $m_x = m_l$  [see Figs. 1 (a) and (b)]. As  $B$  grows, however, valleys 2 and 3 are progressively cooled, whereas valleys 1 are heated. At a threshold magnetic-field strength ( $\simeq 4.5$  T for the case  $E_A=6$  kV/cm considered in Fig. 3) all the valleys exhibit the same average energies and populations. Above such threshold field valleys 2 and 3 (valleys 1) now become the coldest and most populated (the hottest and less populated), which further confirms the effects investigated in Ref. [12]. Concerning

the overall average energy, it can be noticed from Fig. 3(b) that for growing magnetic fields such a quantity exhibits an initial moderate rise (with a maximum increase lower than  $\simeq 5\%$ ) followed by a decrease. This trend can be understood as follows. For weak magnetic fields, valleys 2 and 3 are still the hottest and thus an increase in their population produces a higher average energy. For an intense enough magnetic field, as the effect of the electric field becomes negligible and the Lorentz-force work is null the electron energy reduces to its thermal value, which explains the decrease.

Figs. 2 (a) and (b) show that, while the drift-velocity is enhanced, the variance is lowered by the magnetic field compared to the zero-magnetic-field case, which indicates that the total noise power is significantly attenuated. Therefore, as a simultaneous conductivity enhancement takes place [cfr. Fig. 2(a)] the presence of the magnetic field reduces the relative importance of velocity fluctuations. This result is strengthened by Fig. 2(c) that shows an essentially monotonous decrease of the relative standard deviation  $\sqrt{\langle \delta v^2 \rangle} / v_d$  in the considered magnetic-field range, the reduction being able to be as pronounced as  $\simeq 20\%$ . In short, the application of the magnetic field is able to yield both a more intense and cleaner signal. We believe this is a rather remarkable result.

It is worth pointing out that, as expected, larger magnetic-field strengths are required for growing electric fields in order for such effects to be exhibited, which is witnessed by a comparison between the plots obtained with different values of  $E_A$  in Fig. 2.

In order to shed light on the mechanism behind noise suppression, in Fig. 3(c) we analyze the behaviour of the valley average velocities along the longitudinal direction, i.e. that of the applied electric field ( $x$ -axis). First, notice that such velocities are rather weakly affected by the magnetic field. As in the zero-magnetic-field case, electrons visiting valleys 2 and 3 move faster than those in valleys 1. Nonetheless, the magnetic field induces a significant transfer of electrons from valleys 1 to valleys 2 and 3 [cfr. Fig. 3(a)], which explains why drift velocity is enhanced [cfr. Figs. 2(a) and 3(c)]. At the same time, as valleys 2 and 3 are significantly occupied even in the absence of magnetic field, such a transfer must necessarily yield a reduced average discrepancy between valley velocities and (increased) drift velocity, i.e. suppression of partition noise takes place. It should be pointed out that, unlike in the absence of magnetic field, in a Hall geometry the electron velocity has intrinsic cyclotron oscillations around its average value dictated by the effective masses and the magnetic-field strength (see Sec. 2 and Refs. [2, 4]). It follows that at intense magnetic fields a relevant contribution to variance comes from such oscillations and thus it might be more appropriate in the present case using the terminology “variance of velocity *deviations*”. The effects of cyclotron oscillations therefore compete with those of partition-noise suppression and the velocity variance in Fig. 2(b) results from the interplay between the two. This is likely to be the reason behind the non-monotonous behaviour in Fig. 2(b). Anyway, it appears reasonable concluding that mere velocity *fluctuations* are actually attenuated.

In order to provide further evidence of partition-noise suppression, in Fig. 4 we set

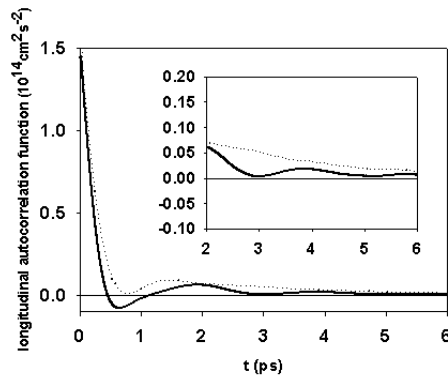


**Figure 4.** Longitudinal autocorrelation function with  $B=4.5$  T (solid line) and in the absence of magnetic field (dotted line). In the insert, a zoom of the time-tale is shown.

$E_A=5$  kV/cm and compare the longitudinal autocorrelation function in the absence of magnetic field (dotted line) with that obtained with a magnetic field  $B=4.5$  T (solid line). As expected [4], in the Hall geometry damped oscillations are exhibited as a signature of cyclotron motion. Nonetheless, the oscillations' center is only slightly above zero. Indeed, a comparison of the time tails with and without magnetic field [see the insert in Fig. 4] shows a magnetic-field-induced attenuation of the long-time-tail effects (remind that these are a well-known signature of partition noise [13, 14, 15]).

#### 4. Conclusions

In summary, in this paper we have investigated how hot-electron noise in n-Si is affected by the presence of a magnetic field in a Hall geometry. In agreement with previous works, we have found that the presence of the magnetic field gives rise to a redistribution of electrons among valleys and enhancement of conductivity. Remarkably, we have found that the drift-velocity enhancement for a given applied electric field occurs with a simultaneous decrease of variance of velocity fluctuations, i.e. the total noise power, and thus of the relative importance of velocity fluctuations. We have shown that such effect results from the magnetic-field-induced transfer of electrons from heavy to light valleys (with respect to the direction of the applied electric field), which causes a significant attenuation of partition noise. We have provided further evidence of partition-noise suppression by comparing the longitudinal autocorrelation functions obtained with and without magnetic field. We have found that the well-known long-time tail effects due to partition-noise are significantly attenuated in the Hall geometry.

In short, it seems reasonable summarizing the results obtained in this work by stating that the magnetic field is able to introduce *order* in the hot-electron dynamics. This circumstance results in a conductive state with higher performances compared to the case where only the electric field is present. We believe the phenomena presented in this work may be attractive in order to design novel strategies for minimizing noise in semiconductor materials exposed to intense electric fields.

Some open questions still remain, such as: What is the optimal Hall geometry for minimizing noise and/or maximizing conductivity? Indeed, it is well-known that in Si, and in general in anisotropic semiconductors, different transport features are obtained with different electric-field geometries. Evidently, when a magnetic field is simultaneously applied, the number of non-trivial Hall geometries giving rise to different conductive regimes is expected to be larger. Indeed, a part of our ongoing work is aimed at establishing the importance of geometry in these phenomena.

Finally, as already mentioned, when quantities such as the variance of velocity fluctuations or the velocity autocorrelation function are computed in a Hall geometry, the outcomes are affected by both mere fluctuations and intrinsic cyclotron oscillations. Therefore, if one is concerned with a mere noise analysis, it would be desirable to filter out somehow the effect of cyclotron motion. The derivation of an appropriate statistical procedure for accomplishing such a task is under ongoing investigations.

## 5. Acknowledgements

The authors are indebted to M G Santangelo (ETH, Zürich) for the help offered in the search of old papers. This work makes use of results produced by the PI2S2 Project managed by the Consorzio COMETA, a project cofunded by the Italian Ministry of University and Research (MIUR) within the Piano Operativo Nazionale "Ricerca Scientifica, Sviluppo Tecnologico, Alta Formazione" (PON 2000-2006).

## References

- [1] Jacoboni C and Reggiani L 1983 *Rev. Mod. Phys.* **55** 645; Jacoboni C and Lugli P 1989 *The Monte Carlo Method for Semiconductor Device Simulation* (Wien: Springer-Verlag); Tomizawa K 1993 *Numerical Simulations of Submicron Semiconductor Devices* (London, Boston: Artech House).
- [2] Boardman A D, Fawcett W and Ruch J G 1971 *Phys. Stat. Sol. (a)* **4**, 133.
- [3] Dijkstra A D 1998 *Appl. Phys. Lett.* **4**, 133 (1998).
- [4] Ciccarello F and Zarcone M 2006 *J. Appl. Phys.* **99** 113702; *Unsolved Problems of Noise and Fluctuations*, ed. by Reggiani L *et al.* 2005 AIP Conf. Proc. **800** 492; *Noise and Fluctuations* ed. by Gonzalez T *et al.* 2005 AIP Conf. Proc. **780**, 159.
- [5] Brazis R S, Starikov E V and Shiktorov P N 1982 *Sov. Phys. Semicond.* **16** 1002.
- [6] Brazis R S, Starikov E V and Shiktorov P N 1983 *Sov. Phys. Semicond.* **17** 8.
- [7] Warmenbol P, Peeters F M, Devreese J T, Alberga G E and van Welzenis R G 1985 *Phys. Rev. B* **31** 5285.
- [8] Warmenbol P, Peeters F M and Devreese J T, *Phys. Rev. B* 1986 **33** 1213.
- [9] Albrecht J D , Ruden P O, Bellotti E and Brennan K F 1999 *MRS Internet J. Nitride Semicond. Res.* 4S1, G6.6.
- [10] Raguotis R A, Repsas K K and Tauras V K 1991 *Lith. J. Phys.* **31** 213; Raguotis R 1992 *Phys. Stat. Sol. (b)* **174** K67.
- [11] Jacoboni C, Minder R and Majni 1975 *J. Chem. Phys. Solids* **36** 1129.
- [12] Asche M and Sarbei O G 1970 *Phys. Stat. Sol.* **37**, 439; Asche M, Bondar V M, Kurtenok L F and Martinchenko V I O G 1973 *Phys. Stat. Sol. (b)* **60** 497.
- [13] Brunetti R and Jacoboni C 1983 *Phys. Rev. Lett.* **50** 1164; Brunetti R and Jacoboni C 1984 *Phys. Rev. B* **29** 5739.



- [14] Brunetti R, Jacoboni C, Nava F, Reggiani L, Bosman G and Zijlstra R J J 1981 *J. Appl. Phys.* **52** 6713.
- [15] Fauquembuergue R, Zimmermann J, Kaszynski A, Constant E and Microondes G J 1980 *J. Appl. Phys.* **51**, 1065.
- [16] Conwell E M and Vassell M O 1968 *Phys. Rev.* **166** 797.